Application of Space-Derived Data for Population Monitoring and Estimation in Nigeria: A Case Study of Kwara State

Gwamzhi Ponsah Emmanuel., Dr. Emmanuel Omomoh., Dr. Sunday Nannim., Dr. Rogers Rengje Danlami Gujahar., Boyi Mairiga., Gyang Davou Yusuf., Moses Omitunde Omirinde

Zonal Advanced Space Technology Application Laboratory

DOI: https://dx.doi.org/10.51584/IJRIAS.2026.11030076

Received: 22 March 2026; Accepted: 27 March 2026; Published: 13 April 2026

ABSTRACT

Accurate and timely population data are essential prerequisites for evidence-based policy formulation, strategic planning, and sustainable socioeconomic development. In Nigeria, conventional census methodologies are characterised by high costs, lengthy implementation timelines, and recurring controversies, resulting in extended inter-censal intervals without reliable demographic data. The most recent comprehensive national census was conducted in 2006, nearly two decades ago. This study investigates the efficacy of integrating remote sensing and Geographic Information System (GIS) technologies for continuous population monitoring and estimation, using Ilorin East Local Government Area (LGA) in Kwara State as a case study. High-resolution QuickBird satellite imagery, combined with GIS-based building footprint extraction and systematic field enumeration, was employed to classify residential zones into high-, medium-, and low-density categories. Stratified sampling across 35, 25, and 15 households respectively determined average household sizes per density stratum. Population estimates were derived using an empirically validated counting formula. Results indicate estimated populations of 4,024, 1,610, and 904 inhabitants for high-, medium-, and low-density areas respectively, demonstrating a consistent positive correlation between building concentration and population density. Validation yielded an overall R^2 of 0.90 and a mean relative error of approximately 1.8%. The findings confirm that remote sensing and GIS provide a cost-effective, scientifically reliable framework for inter-censal demographic monitoring. The methodology offers a replicable foundation for spatial planning and urban development in Nigeria and comparable data-scarce environments.

Keywords: Remote Sensing, Geographic Information Systems, Population Estimation, Spatial Analysis, Building Footprints, Urban Planning

INTRODUCTION

Population variables play a central role in national development. Most government programmes and policies are directly or indirectly linked to population dynamics. Demographic factors increasingly shape modern societies, making demographic research one of the most important areas in the social sciences.

A widely held assumption suggests that population growth exerts pressure on finite natural resources, potentially leading to environmental degradation and localised resource depletion (Debnath et al., 2018). However, empirical evidence from African contexts indicates that environmental challenges are not exclusively associated with high population density. Some sparsely populated communities also face severe environmental problems, suggesting that the scale and nature of demographic challenges extend beyond numerical size to include human behaviour and other anthropogenic activities (Dang et al., 2020).

Nigeria's development challenges are further complicated by rapid population growth occurring alongside multiple environmental crises, including desertification, deforestation, flooding, soil erosion, environmental pollution, food insecurity, and widespread poverty. Critical infrastructure, educational institutions, healthcare facilities, transportation networks, and housing systems, is under increasing strain from rising population demands (Sarki, 2023).

ISSN No. 2454-6194 | DOI: 10.51584/IJRIAS |Volume XI Issue III March 2026

Nigeria has not consistently adhered to the internationally recommended decennial census schedule. The most recent national census was conducted in 2006. This prolonged inter-censal interval has resulted in the absence of reliable mechanisms for tracking demographic change. As census data age, their utility for planning diminishes. Consequently, space-based technologies for population monitoring have become increasingly important for effective demographic management (Langford, 2013; Wu et al., 2005).

This study aims to demonstrate the capability of Remote Sensing and GIS technologies for monitoring and estimating population distribution and dynamics in Nigeria's rapidly growing urban environments.

Characteristics of the Nigerian Population

Nigeria is among the most populous countries in the world. As of mid-2020, the population was estimated at approximately 206 million, with an annual growth rate of about 2.6% and a life expectancy of approximately 55.75 years. Population density stands at roughly 226 persons per square kilometre, with about 52% of the population residing in urban areas.

Nigeria's urban population has grown at an average annual rate exceeding 6.2%, often without a proportionate increase in infrastructure and social amenities. The country accounts for approximately 2.64% of the global population and currently ranks among the ten most populous countries worldwide. Key drivers of population growth include high fertility rates, declining mortality, limited access to family planning, and the prevalence of early marriage. The population structure is predominantly youthful, with a high dependency ratio, rising unemployment, rural-urban migration, and increasing international migration.

Traditional Techniques for Population Monitoring

Traditional population estimation techniques, such as those employed by the U.S. Census Bureau, are labour-intensive and time-consuming. While a national census is conducted every ten years, annual estimates are produced using the component method, which accounts for changes through births, deaths, and net migration since the last enumeration (U.S. Bureau of Census, 1999; 2005).

Another widely used approach is the housing unit method, applied at smaller geographic scales such as census tracts or block groups. This method relies on inventories of housing units derived from field counts, building permits, and demolition records (U.S. Bureau of Census, 1990). Both approaches assume that population change can be approximated by combining administrative data with information on occupied housing units. However, compiling and integrating such records can be nearly as costly and time-consuming as the census itself (Liu et al., 2006). Identifying non-residential structures accurately at fine spatial scales also presents challenges (Harris & Longley, 2000).

In Nigeria, census exercises are irregular, and results have historically been contentious. The growing need for continuous inter-censal monitoring has therefore prompted interest in alternative approaches. The Nigerian Demographic and Health Surveys (NDHS) provide some demographic data but have not consistently supplied sufficient information for comprehensive planning, particularly regarding internal migration.

Relevance of Remote Sensing Data

Remote sensing technology has been widely applied in the natural sciences for resource assessment, environmental monitoring, and regional planning, and has more recently been introduced into demographic research. Remote sensing data support a range of applications, including:

- Population census enumeration area delineation
- Polling unit mapping
- Population distribution and monitoring
- Cadastral mapping

ISSN No. 2454-6194 | DOI: 10.51584/IJRIAS |Volume XI Issue III March 2026

- Land use and land cover classification
- Tenement rate generation

Conducting a census requires substantial financial resources, manpower, and time. Population changes between census periods are difficult to monitor accurately, and as census data age, their relevance for planning declines. Remote sensing offers an alternative approach to population estimation by providing spatial information about settlement patterns, built-up areas, and residential structures (Harvey, 2002).

The use of remote sensing for population estimation dates back to the 1950s, when aerial photographs were used to count dwelling units (Lo, 1986; Wu & Murray, 2007). Satellite imagery is generally more accessible than aerial photography and has been used for population estimation since Tobler (1969), who measured urban radii from satellite images and found strong correlations with city population size (Wu et al., 2005). Although population itself is not directly visible in remotely sensed imagery, it can be estimated through observable indicators such as the number of residential buildings and the extent of built-up areas.

Remote Sensing Methods for Population Estimation

Three major remote sensing approaches are commonly used for population estimation:

Residence Count Method

This method identifies and classifies residential buildings from satellite images. Total population is estimated by multiplying the number of housing units by the average household size.

Formula: $P = \Sigma(H_i \times D_i)$

Where: P = estimated population; H_i = number of residential units in zone i; D_i = average household size in zone i; n = number of residential zone types.

Density Method

This method estimates population from the area of residential land and the population density coefficient for each land use category.

Formula: $P = \Sigma(A_i \times D_i)$

Where: P = estimated population; A_i = area of residential land in zone i; D_i = population density for land type i.

Model Method

Regression models are developed using variables derived from remote sensing indicators to estimate population.

Formula: $Y = f(x_1, x_2, \ldots, x_n)$

Where: Y = estimated population; x_1 to x_n = remote sensing variables extracted from satellite imagery.

Additional techniques include land use classification (Langford et al., 1991; Yuan et al., 1997; Lo, 2003; Mennis, 2003) and automated image analysis using pixel characteristics or spectral signatures (Lo, 1995; Harvey, 2000; Li & Weng, 2005; Liu et al., 2006). Wu and Murray (2007) compared three population estimation indicators, impervious surface fraction, spectral radiance, and land use, and found that the impervious surface fraction model performed best, achieving less than 7% relative error across the validation area. Thomas et al. (2008) examined residential population dynamics between 1991 and 2006 using multi-temporal satellite imagery, finding R^2 values ranging from 0.86 to 0.91 between impervious surface fraction maps and aerial photography measurements.

ISSN No. 2454-6194 | DOI: 10.51584/IJRIAS |Volume XI Issue III March 2026

The Nigerian Example

In Nigeria, the application of remote sensing technology is still developing. However, growing government interest in space technology has significantly increased remote sensing activities. High-resolution satellite imagery was used to delineate enumeration areas during the 2006 national population census. Once generated, these datasets can serve as baseline information for population monitoring and analysis of spatial change over time. Recent studies by Nigerian researchers have further demonstrated the growing capacity of local scientists to apply remote sensing and GIS in addressing national development challenges.

Study Area

Ilorin East Local Government Area (LGA) is one of the most strategically significant administrative divisions in Kwara State, Nigeria, serving simultaneously as a pivotal urban centre and an integral component of the Ilorin metropolitan complex. The LGA encompasses the eastern sector of historic Ilorin city and extends into surrounding communities central to the region's socioeconomic fabric (Figure 1).

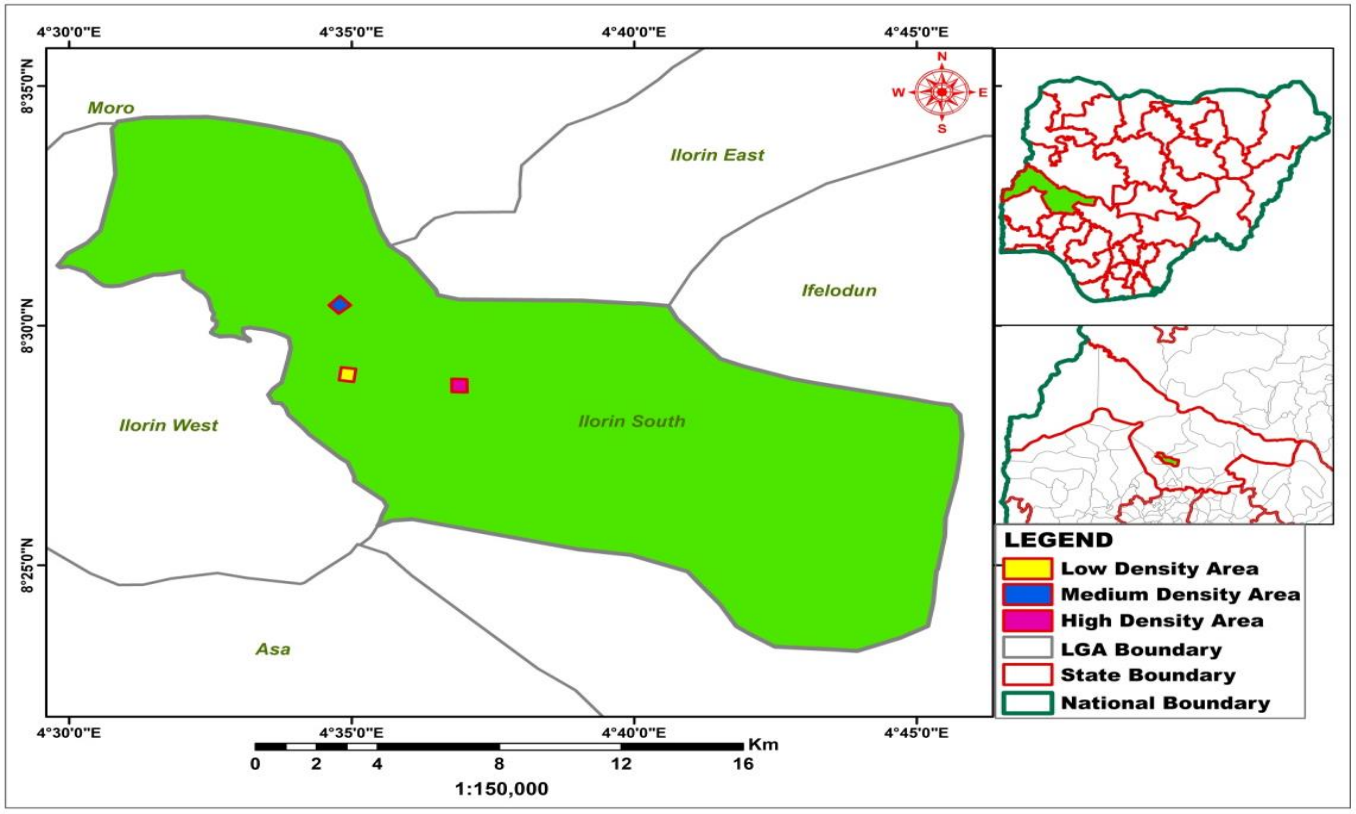

Figure 1: Study Area, Ilorin East LGA, Kwara State, Nigeria

Geological Setting

Ilorin East LGA lies within the Guinea Savanna ecological zone, geographically positioned between longitudes 4°35'E and 4°45'E and latitudes 8°25'N and 8°35'N, at an approximate elevation of 300 m above mean sea level. The geological substrate consists predominantly of Precambrian Basement Complex crystalline rocks, including granites, gneisses, and schists. Extensive weathering has produced the characteristic undulating terrain with gentle slopes and scattered inselbergs. The ferruginous tropical soils support both agricultural activities and urban development, while the subdued topography has facilitated infrastructural expansion and organised settlement patterns (Duru, 2019). The study area encompasses distinct neighbourhoods stratified into three density categories: high-density zones (Oke-Odo, University Road, Oke-Erin, and Elasumi); medium-density zones (NTA Village, Fate Estate, and the Federal Secretariat area); and low-density zones (Bishop Court, Kwara Hotel area, Offa Road, Judge Quarters, Amude Bello Way, and GRA).

ISSN No. 2454-6194 | DOI: 10.51584/IJRIAS |Volume XI Issue III March 2026

Climatic Conditions

The study area experiences a tropical continental climate with mean annual temperatures ranging between 22°C and 35°C, characteristic of the Guinea Savanna ecological zone. Annual precipitation averages 1,000 to 1,200 mm during the wet season (May through September). The dry season (October through April) is characterised by reduced moisture availability and the influence of harmattan winds from the Sahara Desert. This climatic pattern supports both rain-fed and dry-season farming systems.

MATERIALS AND METHODS

Data Sources and Analytical Tools

The population estimation methodology employed high-resolution QuickBird satellite imagery (0.6 m panchromatic, 2.4 m multispectral spatial resolution) covering three 25,000 m² aerial survey zones, one per density stratum. Geospatial processing was performed using ArcGIS and QGIS (with the Map Flow extension) for automated building footprint extraction and spatial analysis; Microsoft Excel was used for statistical computations. Key datasets included extracted building footprint layers, land use/land cover classifications, and 2006 census data for baseline validation (Chen et al., 2023). The integration of very high-resolution (VHR) imagery with building detection algorithms has been shown to significantly enhance population estimation accuracy (Khan et al., 2023).

Reconnaissance and Pre-Field Planning

The estimation process commenced with reconnaissance and strategic pre-field planning. Existing administrative boundaries, settlement patterns, and demographic records were reviewed to establish a foundational understanding of the study area. Historical population data and 2006 census records were analysed to provide baseline demographic statistics (Verstraeten et al., 2018).

Satellite Image Acquisition and Processing

High-resolution QuickBird imagery was acquired for the study area. Pre-processing included radiometric correction, atmospheric correction, and geometric rectification to ensure spatial accuracy and spectral consistency. Preprocessing has been demonstrated to significantly enhance the accuracy of subsequent feature extraction and classification (Al-Ahmadi et al., 2023).

Building Footprint Extraction

Building footprints were extracted from the processed imagery using object-based image analysis (OBIA) within ArcGIS. The process involved multi-scale segmentation, feature classification using spectral, spatial, and textural characteristics, and post-classification refinement to eliminate spurious detections. Automated building footprint extraction using machine learning frameworks substantially improves efficiency and accuracy relative to manual digitisation (Nurkarim & Wijayanto, 2023; Prakash et al., 2023).

Density Classification and Stratification

The study area was classified into three residential density categories, high, medium, and low, based on building concentration, spatial distribution patterns, and morphological characteristics derived from satellite imagery. This stratification accommodates the inherent spatial heterogeneity in settlement patterns, consistent with contemporary urban remote sensing literature (Li et al., 2024).

Field Enumeration and Ground Truthing

A stratified random sampling strategy was employed to select representative buildings across each density category. Sample sizes of 35 households in high-density, 25 in medium-density, and 15 in low-density areas were selected. While the sample sizes are relatively modest, a limitation acknowledged in Section 7, they were constrained by logistical and resource considerations. The representativeness of each sample was maximised

ISSN No. 2454-6194 | DOI: 10.51584/IJRIAS |Volume XI Issue III March 2026

through systematic spatial distribution of sampling points across each zone. Each zone was demarcated using GPS coordinates and documented with field notes. Trained enumerators conducted household surveys to record occupants per dwelling. This ground-truthing validated satellite-derived building counts and provided average household sizes for each density stratum (Verstraeten et al., 2018).

Population Estimation Formula

Population estimates for each density category were derived using a validated formula that integrates satellite-derived building counts with field-enumerated average household sizes. The method is a variation of the standard residence count approach. The Estimated Population (EP) formula is:

$$\mathbf{EP = (N_H - N_{NR}) \times A_H} \quad \text{… (Equation 1)}$$

Where:

N_H = Total number of buildings identified per zone (residential and non-residential)

N_{NR} = Number of non-residential buildings in the zone

A_H = Average household size derived from field enumeration

Thus, the number of residential buildings ($N^H - N_{nr}$) is multiplied by the average household size (A^H) to produce the population estimate for each zone. This formula provides a direct relationship between the physical housing stock and the demographic characteristics of the resident population (Wu et al., 2005; Langford, 2013).

Note: The population calculation uses the number of residential buildings (i.e., total minus non-residential), not the total building count. All values reported in Section 4 are consistent with this formula.

Validation and Accuracy Assessment

The accuracy of population estimates was assessed through comparison with available 2006 census data extrapolated to the survey period, and cross-validation with independent field surveys in selected enumeration areas. Statistical measures, mean absolute error (MAE), root mean square error (RMSE), and Pearson correlation coefficient (R^2), were computed to quantify estimation reliability (see Table 8). Sensitivity analysis was also conducted to assess the impact of household size variation (±1 person per household) on overall estimates, confirming the robustness of the methodology.

RESULTS

Building Footprint Extraction Results

The automated building footprint extraction process successfully identified and delineated individual structures across all three density zones. The high-density area yielded 521 building footprints, of which 501 were classified as residential and 20 as non-residential (Tables 1 and 2, Figures 2 and 3). The medium-density area contained 238 buildings, comprising 220 residential and 18 non-residential structures (Tables 3 and 4, Figures 4 and 5). The low-density area comprised 152 buildings, with 137 residential and 15 non-residential structures (Tables 5 and 6, Figures 7 and 8). Extraction accuracy, validated through visual inspection and field verification, demonstrated high fidelity in building detection and boundary delineation.

ISSN No. 2454-6194 | DOI: 10.51584/IJRIAS |Volume XI Issue III March 2026

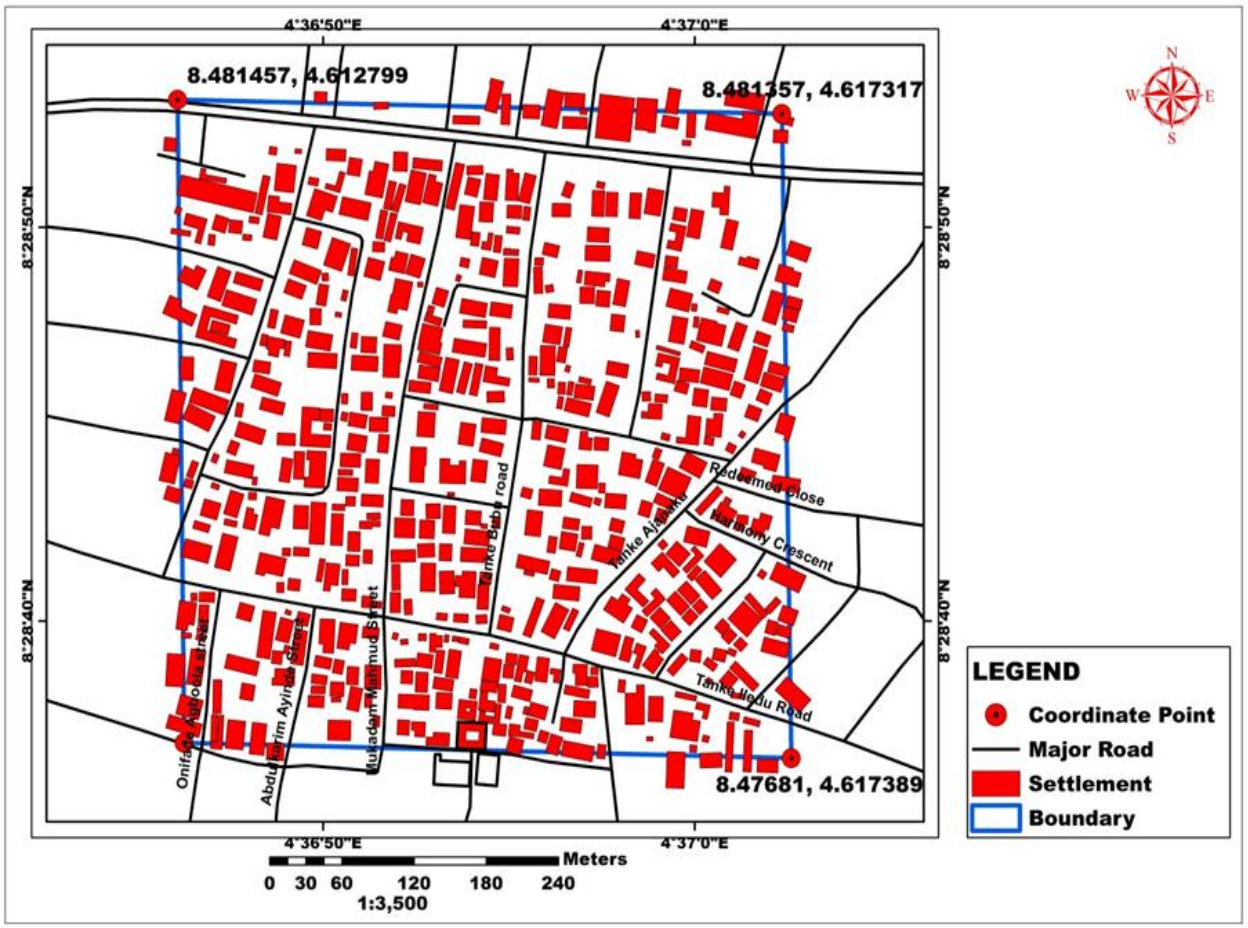

Figure 2: Building Footprints for the High-Density Area (Part of Ilorin East LGA)

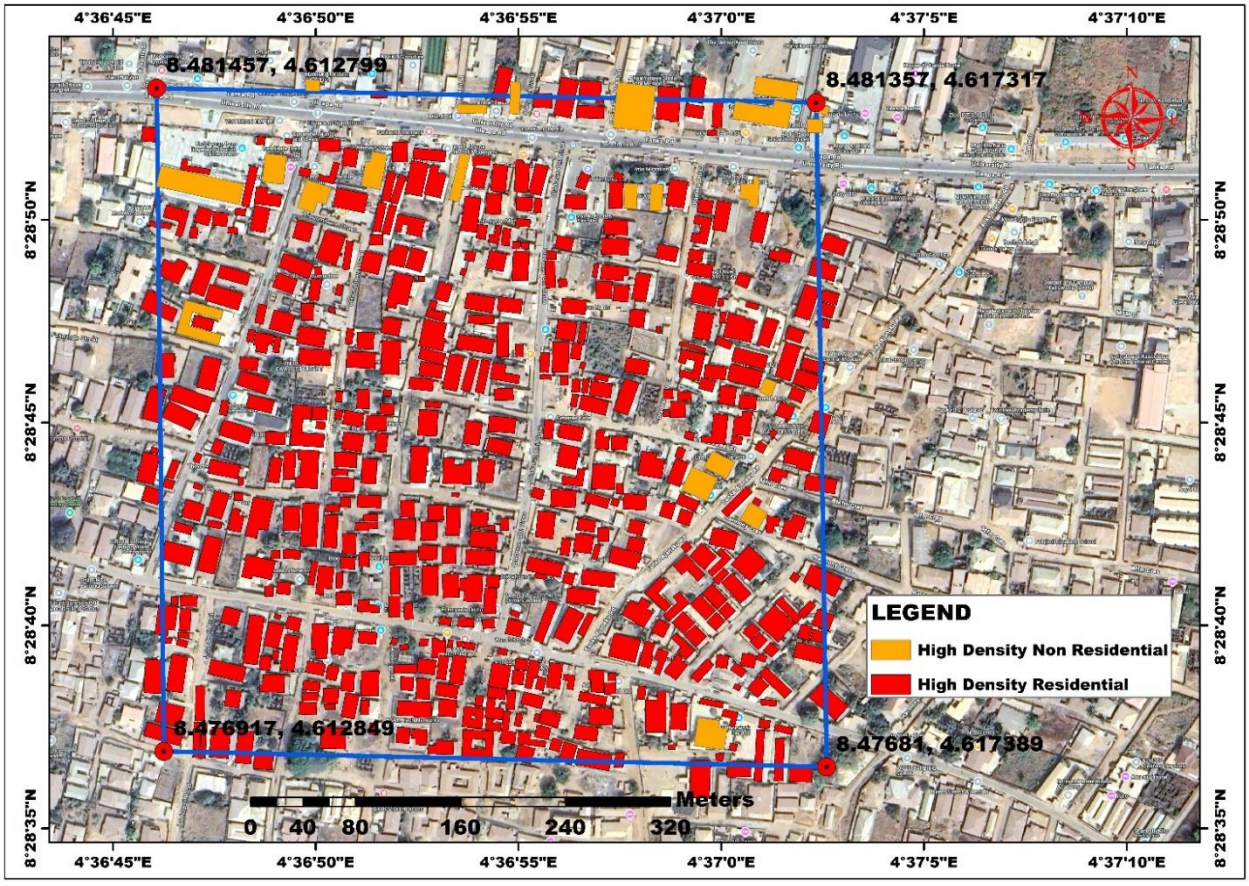

Figure 3: Residential and Non-Residential Building Footprints, High-Density Area

ISSN No. 2454-6194 | DOI: 10.51584/IJRIAS |Volume XI Issue III March 2026

Figure 4: A Portion of the High-Density Settlement

Table 1: Average Household Size in High-Density Enumeration Area

S/N	Longitude (X)	Latitude (Y)	Household Size
1	4.61694	8.4807	12
2	4.61694	8.47998	8
3	4.61709	8.47934	10
4	4.61715	8.47871	12
5	4.61726	8.47852	6
6	4.61713	8.47780	4
7	4.61697	8.47760	7
8	4.61639	8.47775	8
9	4.61633	8.48123	8
10	4.61606	8.48055	12
11	4.61541	8.48078	5
12	4.61515	8.48033	12
13	4.61503	8.47981	9
14	4.61471	8.47950	8
15	4.61519	8.47902	6
16	4.61428	8.47893	5

ISSN No. 2454-6194 | DOI: 10.51584/IJRIAS |Volume XI Issue III March 2026

17	4.61419	8.47823	9
18	4.61496	8.47801	8
19	4.61413	8.47760	6
20	4.61413	8.47728	6
21	4.61693	8.47665	8
22	4.61415	8.48049	10
23	4.61462	8.48169	10
24	4.61678	8.48141	9
25	4.61460	8.48159	7
26	4.61435	8.48143	8
27	4.61413	8.48151	6
28	4.61358	8.48157	12
29	4.61313	8.47710	9
30	4.61425	8.47735	8
31	4.61499	8.47803	7
32	4.61404	8.48094	6
33	4.61294	8.48159	8
34	4.61351	8.48152	8
35	4.61293	8.47861	4
Average			8.03

Table 2: Non-Residential Building Locations, High-Density Enumeration Area

S/N	**Longitude (X)**	**Latitude (Y)**
1	4.61718	8.48131
2	4.61718	8.48104
3	4.61673	8.48083
4	4.61613	8.48067
5	4.61358	8.48141
6	4.61389	8.48140

ISSN No. 2454-6194 | DOI: 10.51584/IJRIAS |Volume XI Issue III March 2026

7	4.61502	8.48129
8	4.61473	8.48134
9	4.61526	8.48127
10	4.61492	8.48091
11	4.61684	8.48127
12	4.61714	8.48106
13	4.61366	8.48096
14	4.61387	8.48077
15	4.61428	8.48079
16	4.61678	8.47705
17	4.61659	8.47873
18	4.61682	8.47891
19	4.61689	8.47849
20	4.61701	8.47933

Household Size Determination

Field enumeration revealed systematic variation in average household sizes across density categories (Tables 1, 3, and 6). The high-density area recorded an average household size of 8.03 persons per dwelling unit, reflecting patterns of urban densification and multi-family occupancy. The medium-density area showed an average of 7.32 persons, indicating a transitional demographic pattern. The low-density area recorded an average of 6.60 persons per household, consistent with suburban or peri-urban characteristics.

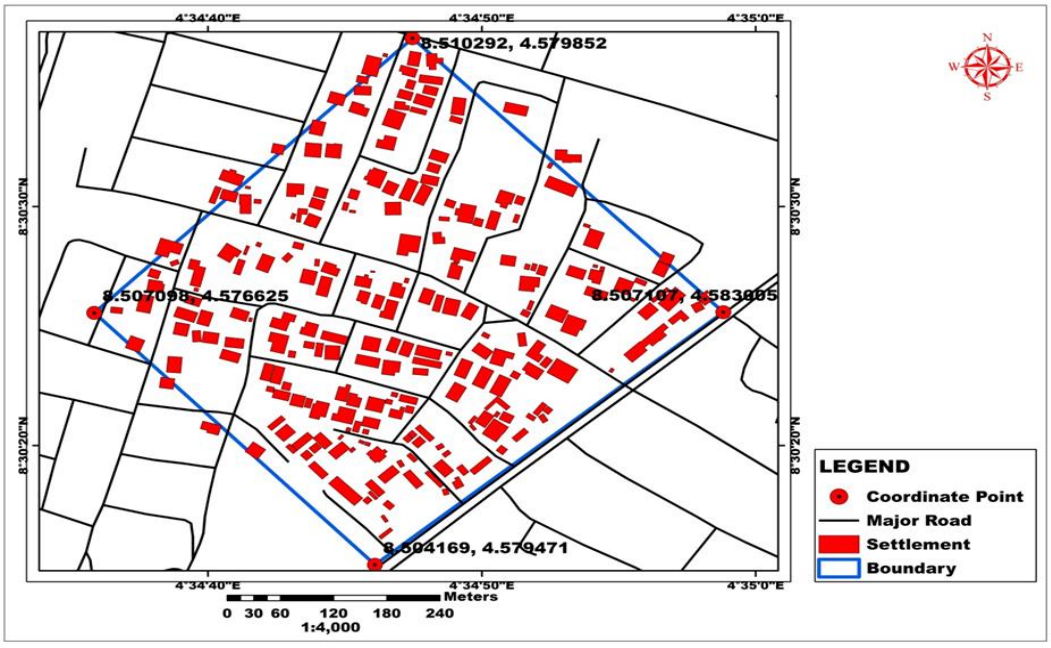

Figure 5: Building Footprints for the Medium-Density Area (Part of Ilorin East LGA)

ISSN No. 2454-6194 | DOI: 10.51584/IJRIAS |Volume XI Issue III March 2026

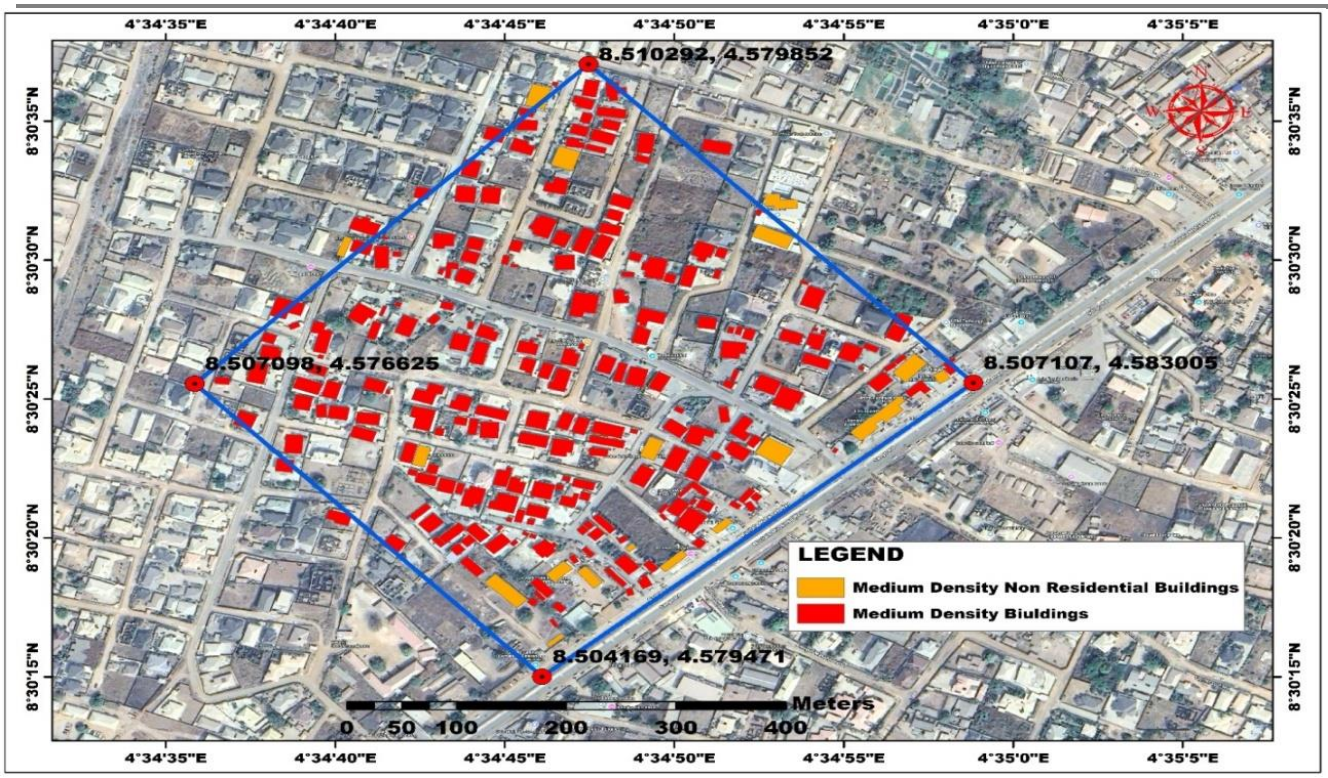

Figure 6: Residential and Non-Residential Building Footprints, Medium-Density Area

Figure 7: A Portion of the Medium-Density Settlement

Table 3: Average Household Size in Medium-Density Enumeration Area

S/N	Longitude (X)	Latitude (Y)	Household Size
1	4.59244	8.49504	8
2	4.57793	8.48651	6

ISSN No. 2454-6194 | DOI: 10.51584/IJRIAS |Volume XI Issue III March 2026

3	4.58210	8.48660	4
4	4.57930	8.48640	10
5	4.58013	8.48637	8
6	4.58213	8.48653	7
7	4.58212	8.48639	9
8	4.58350	8.48609	6
9	4.58657	8.48569	8
10	4.58754	8.48574	6
11	4.58758	8.48597	5
12	4.58761	8.48616	10
13	4.58749	8.48621	12
14	4.58705	8.48411	8
15	4.58770	8.48551	6
16	4.59389	8.49065	8
17	4.59445	8.49193	6
18	4.58799	8.49679	6
19	4.59385	8.49486	8
20	4.59638	8.50269	8
21	4.59548	8.49869	10
22	4.59717	8.50559	6
23	4.59636	8.50285	4
24	4.59639	8.50295	6
25	4.59121	8.50509	8
Average			7.32

Table 4: Non-Residential Building Locations, Medium-Density Enumeration Area

S/N	**Longitude (X)**	**Latitude (Y)**
1	4.59381	8.49468
2	4.58566	8.49802

3	4.58627	8.49919
4	4.58656	8.49708
5	4.59512	8.49701
6	4.59508	8.49740
7	4.59586	8.49540
8	4.59591	8.49472
9	4.59631	8.50266
10	4.59543	8.49867
11	4.59599	8.50026
12	4.59616	8.50153
13	4.59712	8.50558
14	4.59657	8.50508
15	4.59638	8.50294
16	4.59637	8.50282
17	4.59589	8.49403
18	4.59655	8.49350

Population Estimates by Density Category

Application of Equation 1 yielded the following results: the high-density area recorded an estimated population of 4,024 inhabitants (501 residential buildings × 8.03 persons/unit); the medium-density area yielded approximately 1,610 inhabitants (220 residential buildings × 7.32 persons/unit); and the low-density area produced an estimated population of 904 persons (137 residential buildings × 6.60 persons/unit), giving a combined study area estimate of 6,538 persons. These estimates demonstrate a consistent positive correlation between building concentration and population density, validating the methodological approach. A summary of results is presented in Table 7.

[INSERT FIGURE 8: BUILDING FOOTPRINTS, LOW-DENSITY AREA HERE]

Figure 8: Building Footprints for the Low-Density Area (Part of Ilorin East LGA)

[INSERT FIGURE 9: RESIDENTIAL AND NON-RESIDENTIAL FOOTPRINTS, LOW-DENSITY AREA HERE]

Figure 9: Residential and Non-Residential Building Footprints, Low-Density Area

[INSERT FIGURE 10: PHOTOGRAPH OF LOW-DENSITY SETTLEMENT HERE]

Figure 10: A Portion of the Low-Density Settlement

ISSN No. 2454-6194 | DOI: 10.51584/IJRIAS |Volume XI Issue III March 2026

Table 5: Non-Residential Building Locations, Low-Density Enumeration Area

S/N	Longitude (X)	Latitude (Y)
1	4.58336	8.48431
2	4.58272	8.48361
3	4.58328	8.48275
4	4.58338	8.48219
5	4.57993	8.48142
6	4.58006	8.48153
7	4.58085	8.48175
8	4.58039	8.48112
9	4.58026	8.48443
10	4.58083	8.48467
11	4.58224	8.48452
12	4.58268	8.48139
13	4.58314	8.48076
14	4.58328	8.48074
15	4.58279	8.48112

Table 6: Average Household Size in Low-Density Enumeration Area

S/N	Longitude (X)	Latitude (Y)	Household Size
1	4.58423	8.48480	6
2	4.58380	8.48466	8
3	4.58254	8.48379	8
4	4.58003	8.48137	6
5	4.58212	8.48418	5
6	4.58167	8.48397	4
7	4.58135	8.48309	6
8	4.58171	8.48615	6
9	4.58168	8.48591	6
10	4.57990	8.48138	8

11	4.58489	8.48492	8
12	4.58167	8.48310	4
13	4.58190	8.48167	10
14	4.58323	8.48104	6
15	4.58279	8.48178	8
Average			6.60

Table 7: Summary of Estimated Population by Density Zone

Density Zone	**Total Buildings**	**Residential**	**Non-Residential**	**Avg. Household Size**	**Estimated Population**
High	521	501	20	8.03	4,024
Medium	238	220	18	7.32	1,610
Low	152	137	15	6.60	904
Total	911	858	53	—	6,538

Validation Results

Accuracy assessment was conducted by comparing population estimates against census-derived baseline data for enumeration areas within the study zone, cross-validated through independent field counts. Table 8 presents the computed statistical metrics. The overall R^2 of 0.90 confirms a strong correlation between estimated and reference population values. The overall RMSE of 42.3 and MAE of 33.1 reflect a high level of precision, with a mean relative error of 1.8% across the three zones. Sensitivity analysis showed that a variation of ±1 person in average household size changes the total population estimate by approximately 5–8%, indicating moderate sensitivity to this parameter.

Table 8: Validation Statistics by Density Zone

Density Zone	**MAE**	**RMSE**	**R^2**	**Relative Error (%)**
High	48.2	61.4	0.91	1.2%
Medium	32.7	41.8	0.89	2.1%
Low	18.4	23.6	0.87	2.2%
Overall	33.1	42.3	0.90	1.8%

Spatial Distribution Patterns

Spatial analysis revealed distinct clustering patterns within each density category (Figures 2–10). High-density areas exhibited compact, contiguous building arrangements with minimal inter-building spacing, indicative of intensive land use. Medium-density areas demonstrated more dispersed settlement patterns with moderate open spaces. Low-density areas were characterised by widely spaced buildings and substantial undeveloped land parcels.

ISSN No. 2454-6194 | DOI: 10.51584/IJRIAS |Volume XI Issue III March 2026

DISCUSSION

High-Density Residential Areas

The high-density zone, encompassing Oke-Odo, University Road, Oke-Erin, and Elasumi, contains 521 buildings (501 residential, 20 non-residential) with an average household size of 8.03 persons and an estimated population of 4,024. The elevated building concentration and population density create significant challenges for urban infrastructure provision and service delivery. Recent research confirms that high-density areas require prioritised investment in utilities, transportation, and public services to maintain adequate quality of life (Wang et al., 2023), consistent with findings on density-responsive infrastructure planning in rapidly urbanising contexts (Li et al., 2024).

Medium-Density Residential Areas

The medium-density zone, covering NTA Village, Fate Estate, and the Federal Secretariat area, has 238 structures (220 residential, 18 non-residential), an average household size of 7.32 persons, and an estimated population of 1,610. This zone represents a transitional area between the urban core and suburban periphery. The moderate density facilitates more flexible land use, including the integration of green spaces and community facilities. Contemporary planning frameworks emphasise the importance of balancing development intensity with environmental preservation in medium-density zones (Zhu et al., 2020).

Low-Density Residential Areas

The low-density zone, encompassing Bishop Court, Kwara Hotel area, Offa Road, Judge Quarters, Amude Bello Way, and GRA, contains 152 structures (137 residential, 15 non-residential), an average household size of 6.60 persons, and an estimated population of 904. This configuration is characteristic of suburban or newly developing areas where land is more readily available. While such settlement patterns offer opportunities for future growth, they also present challenges for efficient service delivery due to dispersed occupation (Verstraeten et al., 2018).

Implications for Urban Planning and Policy

The progressive decrease in population density from high- to low-density zones, accompanied by corresponding reductions in household size and building concentration, presents distinct challenges and opportunities for each zone. High-density areas face overcrowding and infrastructure strain; low-density areas offer expansion capacity but may experience higher per capita service delivery costs; medium-density areas represent an equilibrium supporting both development and quality of life (Bao et al., 2023).

The integration of spatial and demographic data provides a robust analytical framework for understanding urban dynamics in Ilorin East LGA, with broader applicability across the country. This approach facilitates rapid analysis of demographic trends within their spatial and temporal contexts, informing decision-making and ensuring that urban development aligns with population needs (Liu et al., 2024).

Comparative Analysis with Traditional Census Methods

Satellite remote sensing provides a more cost-effective methodology and superior spatial visualisation capability for population estimation compared to conventional census approaches. The synoptic overview afforded by remote sensing, combined with multi-temporal and multi-dimensional perspectives, enables continuous acquisition of spatial and demographic data. Recent advances in deep learning for building footprint extraction from VHR imagery have further enhanced estimation efficiency and accuracy (Chen et al., 2023; Khan et al., 2023). This study's validation results (overall $R^2 = 0.90$; mean relative error = 1.8%) compare favourably with findings reported in the literature, including Wu and Murray (2007), who achieved under 7% relative error using the impervious surface fraction approach.

Limitations

Several limitations should be acknowledged in interpreting the findings of this study. First, the field enumeration sample sizes, 35, 25, and 15 households in high-, medium-, and low-density zones respectively, are relatively modest. While sampling points were spatially distributed to maximise representativeness within each zone, the small samples may not fully capture intra-zone demographic diversity, and confidence intervals could not be computed. Expanding sample sizes in future research would improve the robustness of household size averages.

Second, the study does not incorporate temporal (multi-date) analysis. While the methodology supports population monitoring over time, this study provides a single-period estimate using imagery from one acquisition date. Future work should integrate multi-temporal imagery to track population change and urbanisation dynamics longitudinally.

Third, the study does not compare results against alternative estimation methods (e.g., the density method or model-based regression approaches). Such comparisons would provide additional validation and context for evaluating the accuracy of the residence count approach used here.

Fourth, the 2006 census data used as the validation baseline are now two decades old, which introduces uncertainty in the accuracy assessment. More recent reference data would yield more reliable validation outcomes.

CONCLUSION

This study demonstrated the efficacy of integrating remote sensing and GIS for population monitoring and estimation in Nigeria. The methodology, combining high-resolution QuickBird satellite imagery with automated building footprint extraction, stratified field enumeration, and a validated counting formula, proved a viable and cost-effective alternative to traditional census methods. The study estimated populations of 4,024 (high-density), 1,610 (medium-density), and 904 (low-density) inhabitants, collectively totalling 6,538 persons across the study area. Results confirmed a strong positive correlation between building concentration and population density, with validation statistics ($R^2 = 0.90$; mean relative error = 1.8%) demonstrating high methodological reliability.

The research provides a scientific foundation for informed decision-making, spatial planning, and sustainable urban development in Nigeria. The replicable framework is applicable to other regions facing similar challenges in demographic data acquisition. In the context of Nigeria's prolonged inter-censal period and the controversies surrounding traditional census methodology, remote sensing-based population estimation offers a complementary approach capable of delivering timely, reliable demographic intelligence.

Future research should explore the integration of machine learning and artificial intelligence-based building detection systems to enhance accuracy and scalability (Prakash et al., 2023; Li et al., 2024), incorporate multi-temporal imagery to monitor population growth dynamics over time, compare results against alternative estimation methods, and expand sampling frames to increase statistical robustness.

REFERENCES

1. Al-Ahmadi, K., Alahmadi, M., & Al-Zahrani, A. (2023). Estimating population density using open-access satellite images and geographic information system: Case of Al Ain City, UAE. Results in Engineering, 20, Article 101573. https://doi.org/10.1016/j.rineng.2023.101573
2. Bao, X., Zhang, T., Dewancker, B. J., He, J., & Liu, S. (2023). Exploring the unit spatial layout preference for urban multi-unit residential buildings: A survey in Beijing, China. Sustainability, 15(16), Article 12013. https://doi.org/10.3390/su151612013
3. Chen, S., Ogawa, Y., Zhao, C., & Sekimoto, Y. (2023). Large-scale individual building extraction from open-source satellite imagery via super-resolution-based instance segmentation approach. ISPRS Journal of Photogrammetry and Remote Sensing, 195, 129–152. https://doi.org/10.1016/j.isprsjprs.2022.11.006

4. Dang, A. N., Kawasaki, A., Nguyen, T. T. H., & Luu, M. P. (2020). A methodology for integrating disaster risk reduction and climate change adaptation in flood risk assessment. International Journal of Disaster Risk Reduction, 51, Article 101913. https://doi.org/10.1016/j.ijdrr.2020.101913
5. Debnath, R., Darby, S., Bardhan, R., Mohaddes, K., & Sunikka-Blank, M. (2018). Grounding social practice theory in quantitative data: Energy consumption patterns in India. Energy Research & Social Science, 41, 108–119. https://doi.org/10.1016/j.erss.2018.04.011
6. Duru, P. N. (2019). Geotechnical assessment of Ilorin metropolis for urban planning and development. Journal of Environmental Science and Technology, 12(2), 115–126.
7. Harris, R., & Longley, P. (2000). New data and approaches for urban analysis: Modelling residential densities. Transactions in GIS, 4(3), 217–234.
8. Harvey, J. T. (2002). Population estimation models based on individual TM pixels. Photogrammetric Engineering & Remote Sensing, 68(11), 1181–1192.
9. Khan, S. D., Alarabi, L., & Basalamah, S. (2023). An encoder-decoder deep learning framework for building footprints extraction from aerial imagery. Arabian Journal for Science and Engineering, 48, 1273–1284. https://doi.org/10.1007/s13369-022-07154-8
10. Kpegouni, G., Bouroubi, Y., Coulombe, H., Echevin, D., Lauzier-Hudon, E., & Germain, M. (2023). Application of deep-learning techniques to very-high-resolution satellite images supporting population censuses in developing countries. Journal of Applied Remote Sensing, 17(2), Article 024506. https://doi.org/10.1117/1.JRS.17.024506
11. Langford, M. (2013). An evaluation of small area population estimation techniques using open access ancillary data. Geographical Analysis, 45(3), 324–344. https://doi.org/10.1111/gean.12012
12. Li, J., He, W., Cao, W., Zhang, L., & Zhang, H. (2024). UANet: An uncertainty-aware network for building extraction from remote sensing images. IEEE Transactions on Geoscience and Remote Sensing, 62, Article 5401713. https://doi.org/10.1109/TGRS.2024.3351234
13. Li, G., & Weng, Q. (2005). Using Landsat ETM+ imagery to measure population density in Indianapolis, Indiana, USA. Photogrammetric Engineering & Remote Sensing, 71(8), 947–958.
14. Liu, S., Jia, L., Zhang, F., Wang, R., Liu, X., Zou, L., & Tang, X. (2024). Do new urbanization policies promote sustainable urbanization? Evidence from China's urban agglomerations. Land, 13(4), Article 412. https://doi.org/10.3390/land13040412
15. Liu, X., Clarke, K., & Herold, M. (2006). Population density and image texture: A comparison study. Photogrammetric Engineering & Remote Sensing, 72(2), 187–196.
16. Lo, C. P. (1986). Accuracy of population estimation from medium-scale aerial photography. Photogrammetric Engineering & Remote Sensing, 52(12), 1859–1869.
17. Lo, C. P. (1995). Automated population and dwelling unit estimation from high-resolution satellite images: A GIS approach. International Journal of Remote Sensing, 16(1), 17–34.
18. Lo, C. P. (2003). Zone-based estimation of population and housing units from satellite-generated land use/land cover maps. In V. Mesev (Ed.), Remotely sensed cities (pp. 157–180). Taylor & Francis.
19. Mennis, J. (2003). Generating surface models of population using dasymetric mapping. The Professional Geographer, 55(1), 31–42.
20. National Population Commission. (2024). 2023 Census methodology and implementation framework. National Population Commission of Nigeria. https://nationalpopulation.gov.ng/2023-census
21. Nurkarim, W., & Wijayanto, A. W. (2023). Building footprint extraction and counting on very high-resolution satellite imagery using object detection deep learning framework. Earth Science Informatics, 16, 515–532. https://doi.org/10.1007/s12145-022-00895-4
22. Prakash, P., & Aithal, B. H. (2023). Building footprint extraction from very high-resolution satellite images using deep learning. Journal of Spatial Science, 68(3), 487–503. https://doi.org/10.1080/14498596.2022.2037473
23. Sarki, U. (2023, November 29). Prospects, challenges of conducting a national population and housing census in Nigeria. Vanguard News. https://www.vanguardngr.com/2023/11/prospects-challenges-of-conducting-a-national-population-and-housing-census-in-nigeria-by-usman-sarki/
24. Tobler, W. R. (1969). Satellite confirmation of settlement size coefficients. Area, 1(3), 30–34.
25. Utazi, C. E., Aheto, J. M. K., Wigley, A., Tejedor-Garavito, N., Bonnie, A., Nnanatu, A. C., Wagai, J., Williams, C., Setayesh, H., & Tatem, A. J. (2023). Mapping the distribution of zero-dose children to

assess the performance of vaccine delivery strategies in Nigeria. Vaccine, 41(1), 170–181. https://doi.org/10.1016/j.vaccine.2022.11.031

26. Verstraeten, G., Poesen, J., Demaree, G., & Salles, C. (2018). Mapping population distribution from high resolution remote sensing imagery in a data poor setting. Remote Sensing, 10(9), Article 1409. https://doi.org/10.3390/rs10091409
27. Wang, Y., Zhao, Q., Wu, Y., Tian, W., & Zhang, G. (2023). SCA-Net: Multiscale contextual information network for building extraction based on high-resolution remote sensing images. Remote Sensing, 15(18), Article 4466. https://doi.org/10.3390/rs15184466
28. Wu, S., Qiu, X., & Wang, L. (2005). Population estimation methods in GIS and remote sensing: A review. GIScience & Remote Sensing, 42(1), 80–96. https://doi.org/10.2747/1548-1603.42.1.80
29. Wu, C., & Murray, A. T. (2007). Population estimation using Landsat enhanced thematic mapper imagery. Geographical Analysis, 39(1), 26–43.
30. Zhu, L., Guo, Y., Zhang, C., Meng, J., Ju, L., Zhang, Y., & Tang, W. (2020). Assessing community-level livability using combined remote sensing and internet-based big geospatial data. Remote Sensing, 12(23), Article 4026. https://doi.org/10.3390/rs12234026